Fibers and Polymers 2019, Vol.20, No.12, 2618-2624
DOI 10.1007/s12221-019-9180-9

ISSN 1229-9197 (print version)
ISSN 1875-0052 (electronic version)

Preparation of Electroconductive, Antibacterial, Photoactive Cotton Fabric Through Green Synthesis of ZnO/reduced Graphene Oxide Nanocomposite

Ali Nazari*

Department of Art & Architectural, Yazd Branch, Islamic Azad University, Yazd 8915813135, Iran

(Received February 19, 2019; Revised June 6, 2019; Accepted June 8, 2019)

Abstract: In this study, a simple and environment friendly approach was used to prepare the multifunctional composite fabrics via coating ZnO/reduced graphene oxide nanocomposite on the surface of cotton without any chemical reducing agent. Graphene oxide was coated on to commercial cotton fabric by dipping the fabric in graphene oxide solution and drying in an oven. The nanocomposite was synthesized on cotton fabric in a single step by reduction of zinc acetate and graphene oxide with pomegranate juice in the impregnation bath. X-ray diffraction spectroscopy, X-ray photoelectron spectroscopy, field emission scanning electron microscopy and energy dispersive spectroscopy confirmed the successful formation of ZnO/graphene nanocomposite on the fabric surface. The treated fabric had superior photocatalytic property in methylene blue degradation, and had excellent antibacterial activity against *Escherichia coli* and *Staphylococcus aureus* bacteria. Furthermore, the electrical resistance of coated fabrics was decreased significantly by the presence of reduced graphene oxide on the surface of cotton fabrics.

Keywords: ZnO/reduced graphene oxide nanocomposite, Cotton, Photoactive, Antibacterial, Electroconductive

Introduction

Several industries like medicine, food, textile, paper, cosmetics, electronic and sensor use zinc oxide nanoparticles as a major source due to its unique characteristics, such as optical and electronic properties, low cost, abilities to purify pollutions, and antimicrobial activity [1-6]. The use of ZnO nanoparticles for functional finishing of textiles has been studied by various groups. Mohammadi and co-workers prepared photoactive and antibacterial fabric through *in situ* synthesis of nano ZnO on polyester fabric [7]. Behzadnia *et al*. produced self-cleaning wool fabric using zinc oxide nanoparticles [8]. Prasad and colleagues obtained durable antibacterial and UV protection fabric based on zinc oxide coatings on cotton fabrics [9]. Zhang *et al*. applied ZnO nanoparticles for generation of antimicrobial bamboo pulp fabric [10].

During the past years, some studies attempted to improve the properties of textiles via the combination of ZnO with other nanomaterials. For instance, Avazpour and colleagues treated cellulose fabrics with Ag/ZnO nanocomposite and reported the significant improvement in self-cleaning and antibacterial properties of the fabric [11]. Along the same lines, Aladpoosh and Montazer produced cellulosic fabric with superior photocatalytic activity using star-like Ag/ZnO nanocomposites [12]. Behzadnia *et al*. improved the self-cleaning, UV-blocking and antimicrobial properties of wool fabric through adding titania to zinc oxide nanoparticles [13]. A chemical coating of cotton with polypyrrole-zinc oxide-carbon nanotube nanocomposites with flame-retardancy and UV blocking properties was reported by Yazhini and Prabu [14]. Also, they used ZnO-CNT for antibacterial finishing of cotton fabrics. The ZnO-CNT-coated fabric has improved antibacterial activity when compared with the ZnO-coated fabric [15]. Moreover, Barani synthesized ZnO/SiO_2 nanocomposites on cotton fabric and obtained antibacterial fabric with excellent performance [16].

Recently, the application of metal or metal oxide/graphene nanocomposites for fabric finishing has also been reported and has shown its advantages [17-24]. Deposition of TiO_2/graphene nanocomposites on textiles provides new properties such as electrical conductivity, self-cleaning, UV protection, antibacterial and antifungal [17-19]. Also, using SnO_2/graphene nanocomposite for electrical conductivity and ultraviolet blocking [20], Ag/graphene nanocomposite for electrical conductivity and antimicrobial [21-24], Fe_3O_4/graphene nanocomposite for magnetism and antibacterial [25] was reported.

Several physical and chemical methods have been proposed to fabricate ZnO/graphene nanocomposite including solvothermal [26], microwave-assisted non-aqueous [27], chemical vapor deposition [28], sol-gel [29], and hydrothermal [30,31]. Through adding graphene on the ZnO, its demerits can be reduced. Graphene would act as an electron acceptor of the photo-generated electrons for ZnO, contributing to the extension of recombination time for electron-hole pairs [32]. Also, the graphene's high surface area would improve the photocatalystic performance of zinc oxide nanoparticles by expanding the photosensitivity under visible light [26,33]. In this work, for the first time the zinc oxide/reduced graphene oxide nanocomposites were synthesized on cotton fabrics based on a green approach. The photo-activity, electrical conductivity and antibacterial activity of the coated fabrics, and the synergism effect of ZnO nanoparticles and graphene on these properties were investigated and are discussed in detail.

---

*Corresponding author: a.nazari@iauyazd.ac.ir

Experimental

Materials

The bleached plain-weave 100 % cotton fabric with the fabric weight of 110 g/m^2 was supplied by Yazbaf Co. (Iran). Pomegranates were purchased from a local market in Yazd, Iran. Graphite powder with particle size less than 20 μm was prepared from Sigma-Aldrich. Zinc acetate dehydrate ($Zn(CH_3COO)_2{\cdot}2H_2O$) as a precursor to synthesis nano ZnO, sulfuric acid (H_2SO_4, 98 %), hydrochloric acid (HCl, 37 %), hydrogen peroxide (H_2O_2, 30 %), potassium permanganate ($KMnO_4$) and methylene blue (CI 52015) were obtained from Merck Co. (Germany).

Synthesis of Graphene Oxide

The improved Hummer method to oxidize graphite for the synthesis of graphene oxide was applied [17]. First, 1 g graphite powder was added to 50 m*l* sulfuric acid under stirring for 12 h at ambient temperature. then, $KMnO_4$ (3.5 g) was slowly put in an ice bath below 10 °C and then stirred for 2 h at 50 °C. After this, deionized water (70 m*l*) and hydrogen peroxide (5 m*l*) were added, and the solution was stirred for 30 min. The resultant product was centrifuged and washed successively with deionized water, 5 % hydrochloric acid and deionized water again (three times). The obtained brown paste was mixed with water, and then the dispersion was sonicated in an ultrasonic bath (WiseClean, 50-60 Hz) for 60 min. The final sonicated dispersion was centrifuged at 3000 rpm for 30 min and the nonexfoliated graphite oxide removed, resulting in a pure graphene oxide aqueous dispersion. Finally, the graphene oxide powder was obtained by freeze-drying.

Preparation of ZnO/reduced Graphene Oxide Nanocomposite on Cotton Fabrics

For coating cotton fabrics with graphene oxide, cotton fabrics were immersed in the aqueous suspension of graphene oxide (0.5 %, wt./wt.) and were heated for 30 min at 80 °C. Then, the fabric was dried in an oven at 85 °C for 20 min. Next, zinc acetate with various concentrations (1, 2, 3, 4 and 5 % wt.) were dissolved in 100 m*l* distilled water at ambient temperature under vigorous stirring. The graphene oxide coated samples or raw cotton samples were immersed into the solutions, and then 40 m*l* of pomegranate juice was added. The solution was stirred at 85 °C for 60 min. The treated fabrics were dried at 60 °C for 30 min followed by curing at 130 °C for 4 min. Finally, the coated fabrics were washed with distilled water and dried at air.

Characterization of Cotton Fabrics

The cotton fabrics were sputtered with gold, and surface morphology and elemental composition were examined by an energy dispersive spectrometer-field emission scanning electron microscope (FE-SEM, MIRA3 TESCAN, Czech). The X-ray diffraction (XRD) patterns of cotton fabrics were obtained using an INEL (model EQuinox 3000) X-ray diffractometer. The X-ray photoelectron spectra were collected and recorded with an X-ray 8025-BesTec XPS system (Germany) with an Al Kα X-ray source ($h\upsilon$=1,486.6 eV).

Test Methods

The photocatalytic efficiency of cotton fabrics was determined in the methylene blue aqueous solution. The samples (4 cm×4 cm) were putted into the beaker which contained 40 m*l* methylene blue aqueous solution (5 mg/*l*) and placed under UV light source (HPA 400 W lamp, Philips, Belgium) for 4 h under continuous stirring (100 rpm). The concentration of dye in the solution was calculated by Varian Cary 300 UV-vis spectrophotometer using calibration curve. The degradation degree of the methylene blue was calculated according to equation (1).

$$\text{Degradation percentage (\%)} = (C_0 - C_e)/C_0 \qquad (1)$$

Here, C_0 and C_e correspond to the initial and final concentration of dye before and after UV irradiation. The degradation percentage values were averaged from five measurements.

AATCC 100-2004 test method was selected as a quantitative technique for measuring antibacterial properties of treated samples against *Escherichia coli* (*E. coli*, ATCC 25922) and *Staphylococcus aureus* (*S. aureus*, ATCC 25923) as ordinary pathogenic bacteria. This method is specially designed for specimens treated with nonreleasing antibacterial agents under dynamic contact conditions. Antibacterial activity was expressed in terms of percentage reduction of micro-organisms and calculated as:

$$\text{Percentage reduction of micro-organisms (R)\%} = (A - B)/A \times 100 \qquad (2)$$

where *A* and *B* are the number of micro-organisms colonies on untreated and treated fabrics, respectively.

There was 3.4×10^5 colony forming units (cfu) of bacteria in primary inoculum. Saline solution 8.5 g/*l* sodium chloride to 1000 m*l* distilled water was used as neutralizing solution. Serial dilution of 10-10,000 was made for incubation on agar plate. Tryptic soy agar (Merck, Germany) was applied as the agar.

Surface resistance of the fabrics was determined based on AATCC test method 76-2005 by means of the Sairan Digital Multimeter, model 8515, Iran.

Results and Discussion

The coating of ZnO/reduced graphene oxide nanocomposite on the cotton fabric was conducted in two steps. First, graphene oxide was placed on cotton surface through dip coating. Then, synthesis of zinc oxide nanoparticles was carried out along with the reduction of graphene oxide using

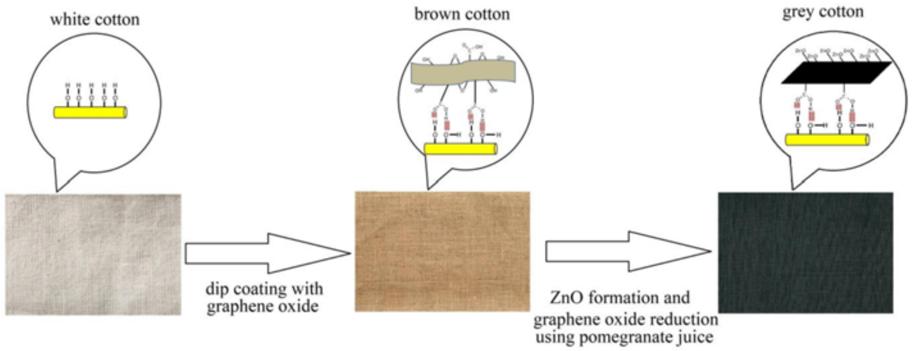

Figure 1. Schematic of step by step preparation of ZnO/reduced graphene oxide nanocomposite on cotton fabric.

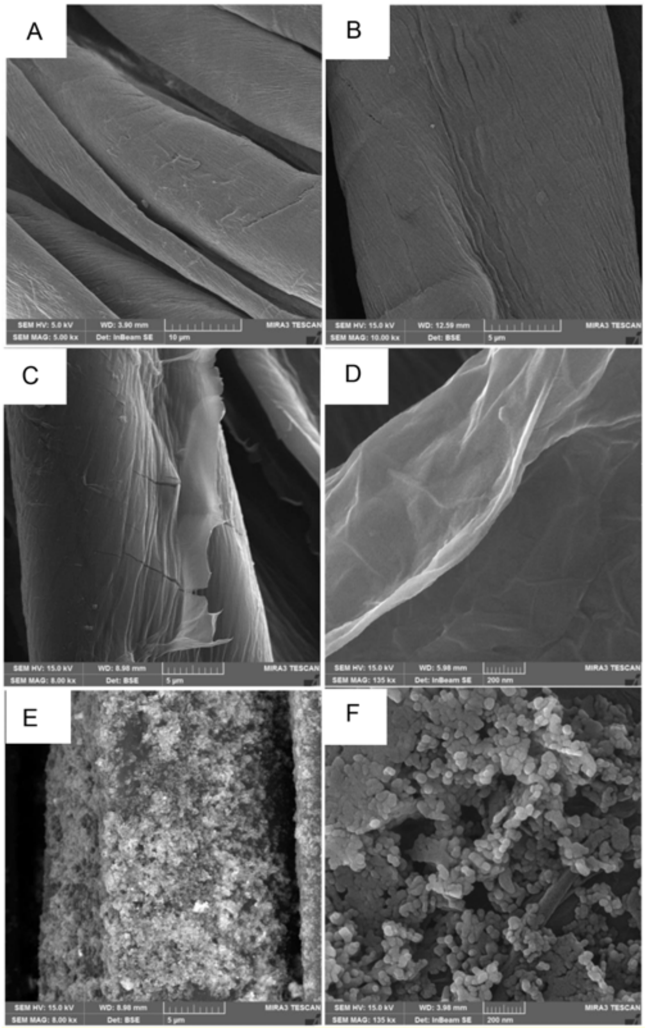

Figure 2. FE-SEM images of various cotton fabrics; (A, B) raw, (C, D) treated with graphene oxide, and (E, F) treated with ZnO/reduced graphene oxide nanocomposite (3 % wt. zinc acetate).

pomegranate juice. The schematic representation of this experiment is exhibited in Figure 1. The cotton fabric adsorbs the graphene oxide sheets into the graphene oxide suspension by forming hydrogen bonds. In previous works, the hydrogen bonding interaction between the oxygen groups on graphene oxide and the hydroxyl groups in the cellulose has been confirmed [34,35]. The pomegranate juice was used as a natural reducing agent to reduce graphene oxide and zinc acetate to synthesize ZnO/reduced graphene oxide nanocomposite on cotton surface. Pomegranate juice is a rich source of several polyphenols [36]. These phenolic compounds act as reducing agents leading to the formation of zinc oxide nanoparticles and the reduction of graphene oxide [37]. Therefore, the fabric color changed from brown to gray, which indicated the reduction of oxygen functional groups from the graphene oxide.

Microscopic images of various cotton fabrics are provided and presented in Figure 2. FE-SEM images revealed that the cotton fabric fiber surface morphology changed after graphene oxide deposition. The treated cotton fabric with a graphene oxide surface displayed some corrugations (Figure 2(C, D)), while the surface of blank cotton fabric was clean and smooth (Figure 2(A, B)). The graphene oxide nanosheets are uniformly coated onto the fibers over the entire fabric and connected together produced a continuous layer on the fabric. After simultaneous graphene oxide reduction and nano ZnO nucleation on cotton fabric, the surfaces of the treated fabric were completely coated by ZnO/reduced graphene oxide nanocomposite condensed to a layer (Figure 2(E)). The ZnO nanoparticles loaded on the surface of reduced graphene oxide nanosheets on the cotton surface with a uniform size. The image at higher magnification (Figure 2(F)) indicate that the reduced graphene oxide nanosheets are decorated with zinc oxide nanoparticles.

Figure 3(A) shows EDS pattern of the sample coated with ZnO/reduced graphene oxide nanocomposite. The strong signals from Zn atoms confirm the presence of zinc oxide particles on the cotton fabric. The presence of Au element in this pattern is due to the gold layer covered the treated sample to prepare for FE-SEM and EDS analysis. Also, X-ray mapping images revealed the good distribution of ZnO nanoparticles on the surface of cotton fabrics (Figure 3(B)).

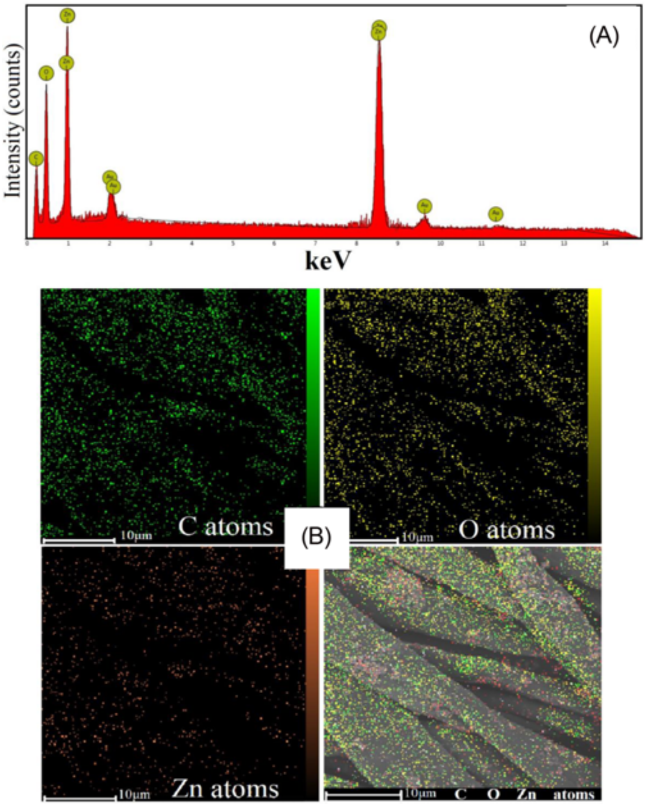

Figure 3. EDS spectrum (A) and X-ray mapping images (B) of treated cotton fabric with ZnO/reduced graphene oxide nanocomposite (3 % wt. zinc acetate).

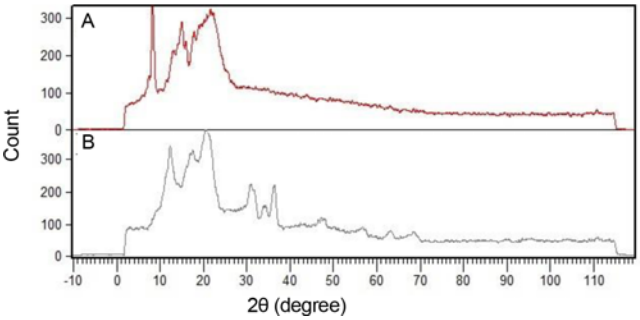

Figure 4. XRD patterns of cotton samples; (A) raw and (B) treated with ZnO/reduced graphene oxide nanocomposite (3 % wt. zinc acetate).

The presence of zinc oxide on the fabric surface could be investigated by XRD patterns. The raw cotton fabrics showed main characteristic diffraction peaks at 13 °, 16.8 ° and 22.6 °, which consisted the typical XRD spectra of cellulose I (Figure 4(A)) [38]. In the case of ZnO/reduced graphene oxide nanocomposite treated fabric (Figure 4(B)), there are seven new peaks at 31.9 °, 34.6 °, 36.5 °, 47.7 °, 56.8 °, 63.1 °, and 67.1 °, corresponding to the (100), (002), (101), (102), (110), (103), and (202) planes of wurtzite zinc oxide (JCPDS Card No. 36-1451). Also, no obvious diffraction peaks of graphene can be seen, indicating the absence of layer-stacking regularity or the relatively low content of graphene on the cotton surface [17].

Wide-scan survey XPS spectra are used to examine the chemical compositions of treated cotton fabric surface, as shown in Figure 5(A). We can find that graphene oxide treated cotton is composed of C and O elements. For nanocomposite treated sample, XPS signal from Zn is detected, indicating a successful zinc oxide deposition onto the fabric surface. To further confirm the surface modification process of the cotton fabric, high-resolution C 1s and Zn 2p peaks of XPS spectra are presented. Figure 5(B) clearly shows that the O/C ratio in the ZnO/reduced graphene oxide nanocomposite treated fabric decreases remarkably compared with that of the graphene oxide treated fabric, and that most of the oxygen groups were successfully removed. Therefore, it be inferred that the graphene oxide was effectively reduced by pomegranate juice. In the Zn 2p spectrum (Figure 5(C)), the peaks for Zn 2p3/2 and Zn 2p1/2 were observed at 1022 eV and 1044.9 eV, which is also indicative of the formation of zinc oxide. Consequently, the results established the successful preparation of the ZnO/reduced graphene oxide nanocomposite on fabric surface.

Figure 6 displayed the degradation degree (D%) of methylene blue dye solution after UV irradiation for the cotton fabric samples. The photolysis of the raw cotton on methylene blue was closed to 0-2 % while ZnO treated fabrics and nanocomposite treated fabrics had good photocatalytic property with 50-100 % degradation percentage after 4 h UV irradiation. The results acquired indicated that increasing the concentration of zinc acetate in the impregnating bath increased the degradation rate of the dye solution. By increasing the concentration of zinc oxide, the amount of generated active oxygen species increased, which led to a better discoloring. Moreover, D% values of the nanocomposites-treated cotton fabrics were more than of the nano-ZnO-treated cotton fabrics. When zinc oxide was illuminated with $\lambda<390$ nm light, active electrons (e^-) and positive holes (h^+) were generated in the conduction band and the valence band of the photocatalyst, respectively. Electron-hole pairs rapidly recombine on the surface or in the bulk of photocatalysts [39]. In the case of ZnO/reduced graphene oxide nanocomposite, photo-induced electrons easily transfer from the ZnO conduction band to reduced graphene oxide, which could efficiently separate the photo-induced electrons and hinder the charge recombination in electron-transfer processes, and thus enhance the photocatalytic performance. Furthermore, the adsorption of dye molecules by reduced graphene oxide nanosheets is helpful for the increase of photocatalytic activity [40-42].

The antibacterial activities of the samples were evaluated quantitatively by suspension method against both *E. coli* and

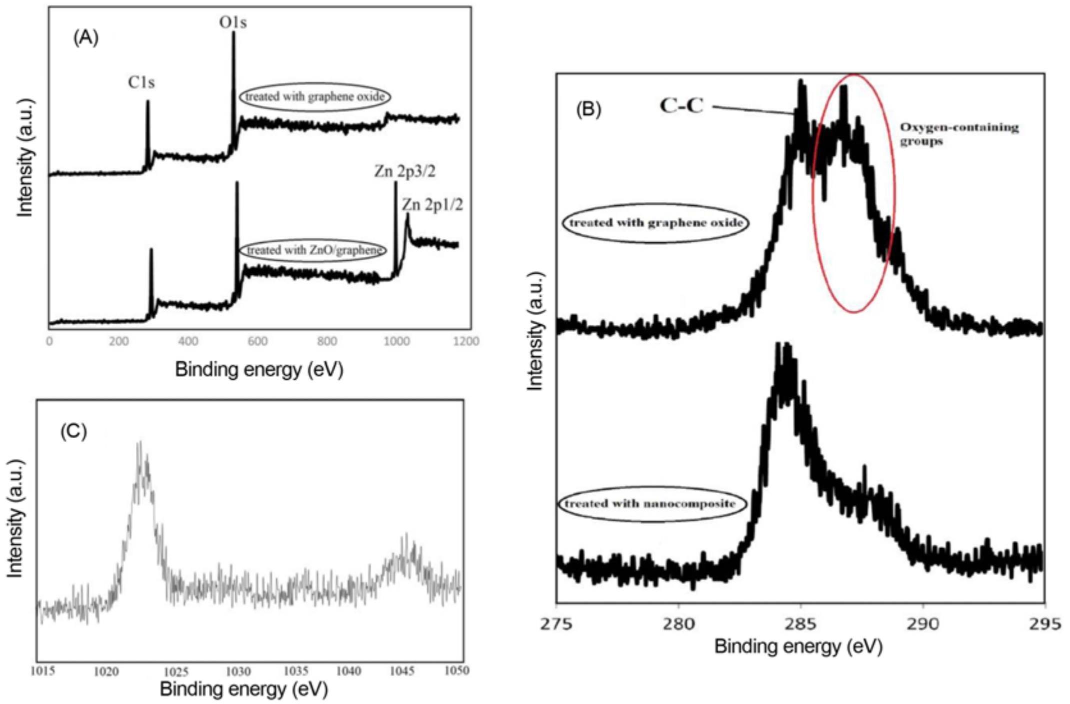

Figure 5. XPS spectra of treated cotton fabrics; (A) survey and (B) C 1s core level. (C) Zn 2p core level spectrum of treated cotton with ZnO/reduced graphene oxide nanocomposite (3 % wt. zinc acetate).

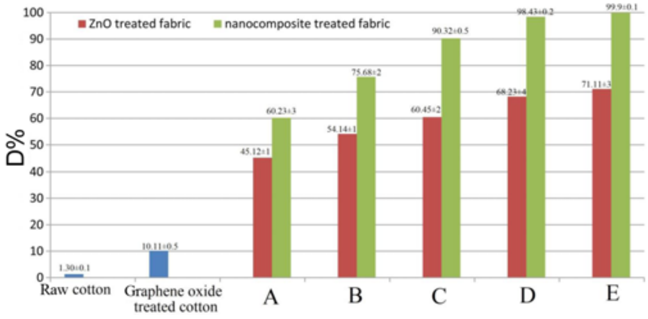

Figure 6. Photocatalytic activity of cotton fabric samples; (A) 1 % wt. zinc acetate, (B) 2 % wt. zinc acetate, (C) 3 % wt. zinc acetate, (D) 4 % wt. zinc acetate, and (E) 5 % wt. zinc acetate.

S. aureus bacteria (Figure 7). There were a number of colonies of viable bacteria seen on agar plates of the blank cotton. The results of quantitative antibacterial activity of reduced graphene oxide treated cotton test shows 61 % antibacterial reduction against *S. aureus* and 70 % against *E. coli*, respectively. The nano-ZnO-treated cotton sample exhibited 66 % of reduction for *S. aureus* and 73 % of reduction for *E. coli*. The ZnO/reduced graphene oxide nanocomposite treated cotton indicated higher antibacterial activity than nano-ZnO or reduced graphene oxide treated fabrics. The nanocomposite treated sample exhibited 100 % of reduction for both *S. aureus* and *E. coli*. The bacteriostatic activity of reduced graphene oxide coated cotton is attributed to either physical interaction with the bacteria or oxidative stress of the cell membranes that disrupts the membranes integrity [43-45]. The ZnO treated textile can inhibit the growth of bacteria possibly by two mechanisms. The first important reason is the production and penetration of reactive oxygen species. The hydroxyl radical and hydrogen peroxide can penetrate into the cell membranes which lead to the death of bacteria. The second reason is of Zn^{2+} ions in the bacterial culture. These positive ions react with negatively charged at the cell surface of microorganism causing a variation of cell permeability, transforming normal metabolism of microorganisms leading to microorganism death [7]. These mechanisms of reduced graphene oxide and ZnO nanoparticles complemented each other and resulted in the significant antibacterial activity of the ZnO/reduced graphene oxide nanocomposite on cotton fabric [46].

The electrical conductivity of the prepared fabric specimens was also investigated. The variation in electrical resistance values of cotton samples are reported in Table 1. The blank cotton and graphene oxide treated cotton were not electroconductive. After reduction of graphene oxide coated cotton fabrics by pomegranate juice, the insulated fabric turned electrical conductive (electrical resistivity in the range of 3.4×10^3-8.2×10^3 Ω sqr^{-1}), which indicated the effective reduction of oxygen functional groups from the graphene oxide. In previous works, similar results were also

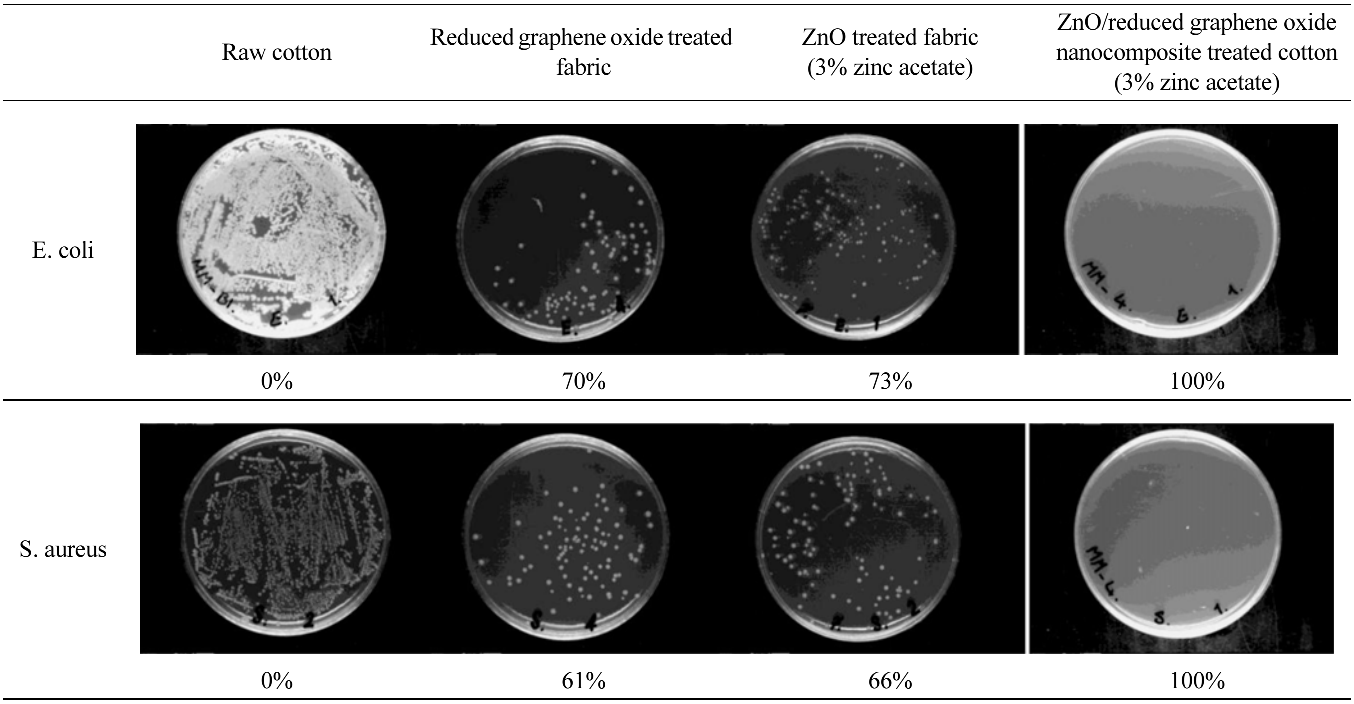

Figure 7. Antibacterial efficiency of the cotton samples.

Table 1. Electrical resistance of various cotton samples

Sample	Zinc acetate (% wt.)	Electrical resistivity (Ω sqr^{-1})
Raw cotton	-	1.1×10^9
Graphene oxide treated cotton	-	2×10^9
Reduced graphene oxide treated cotton	-	3.4×10^3
Nanocomposite treated cotton	1	3.6×10^3
Nanocomposite treated cotton	2	4.1×10^3
Nanocomposite treated cotton	3	6.4×10^3
Nanocomposite treated cotton	4	7.9×10^3
Nanocomposite treated cotton	5	8.2×10^3

reported on the reduction of graphene oxide coated cotton fabrics by different chemical reducing agents, such as $NaBH_4$, N_2H_4, $C_6H_8O_6$, $Na_2S_2O_4$ and NaOH [47,48]. Also, the electrical resistance of nanocomposite treated fabrics increased from 3.6×10^3 Ω sqr^{-1} to 8.2×10^3 Ω sqr^{-1} by increasing the amount of zinc acetate from 1 to 5 wt. %. The condensed deposition of nano-ZnO results in charge transfer to the graphene and a reduction of graphene mobility by charged impurity scattering [49].

Conclusion

In summary, a multifunctional cotton fabric with high photo-activity, excellent antibacterial activity and electro-conductivity has been fabricated by green deposition of ZnO/reduced graphene oxide nanocomposite on the fabric surface. It was observed that adding reduced graphene oxide to zinc oxide nanoparticles could significantly improve the photocatalytic self-cleaning and antibacterial properties of the treated fabrics. In addition, the existence of reduced graphene oxide on the fabric surface caused high electrical conductivity. Our design starts from simple chemistry, and may offer a versatile and scalable approach to fabricate multifunctional fabrics for industrial and healthcare applications, including but not limited to textiles, packaging, public health settings and surgical equipment.

References

1. A. Kołodziejczak-Radzimska and T. Jesionowski, *Materials*, **7**, 2833 (2014).
2. X. Yang, C. Zhang, A. Li, J. Wang, and X. Cai, *Mater. Sci. Eng. C*, **95**, 104 (2019).
3. S. Ni, H. Zhang, P. M. Godwin, H. Dai, and H. Xiao, *Mater. Lett.*, **230**, 207 (2018).
4. M. Z. Khan, V. Baheti, M. Ashraf, T. Hussain, A. Ali, A. Javid, and A. Rehman, *Fiber. Polym.*, **19**, 1647 (2018).
5. P. J. Lu, S. C. Huang, Y. P. Chen, L. C. Chiueh, and D. Y. C. Shih, *J. Food Drug. Anal.*, **23**, 587 (2015).
6. X. Liu, Y. Yang, X. Xing, and Y. Wang, *Sensor Actuat B-Chem.*, **255**, 235 (2018).
7. M. Mohammadi, L. Karimi, and M. Mirjalili, *Fiber. Polym.*, **17**, 1371 (2016).

8. A. Behzadnia, M. Montazer, and M. M. Rad, *J. Photochem. Photobiol. B*, **149**, 103 (2015).
9. V. Prasad, A. Arputharaj, A. K. Bharimalla, P. G. Patil, and N. Vigneshwaran, *Appl. Surf. Sci.*, **390**, 936 (2016).
10. G. Zhang, Y. Liu, H. Morikawa, and Y. Chen, *Cellulose*, **20**, 1877 (2013).
11. S. Avazpour, L. Karimi, and S. Zohoori, *Coloration Technol.*, **133**, 423 (2017).
12. R. Aladpoosh and M. Montazer, *Carbohydr. Polym.*, **141**, 116 (2016).
13. A. Behzadnia, M. Montazer, and M. M. Rad, *Ultrason. Sonochem.*, **27**, 10 (2015).
14. K. B. Yazhini and H. G. Prabu, *RSC Adv.*, **5**, 49062 (2015).
15. K. B. Yazhini and H. G. Prabu, *Appl. Biochem. Biotechnol.*, **175**, 85 (2015).
16. H. Barani, *Appl. Surf. Sci.*, **320**, 429 (2014).
17. L. Karimi, M. E. Yazdanshenas, R. Khajavi, A. Rashidi, and M. Mirjalili, *Cellulose*, **21**, 3813 (2014).
18. M. A. Shirgholami, L. Karimi, and M. Mirjalili, *Fiber. Polym.*, **17**, 220 (2016).
19. L. Karimi, M. E. Yazdanshenas, R. Khajavi, A. Rashidi, and M. Mirjalili, *Appl. Surf. Sci.*, **332**, 665 (2015).
20. V. Babaahmadi and M. Montazer, *Colloids Surf. A Physicochem. Eng. Asp.*, **506**, 507 (2016).
21. V. Babaahmadi, M. Montazer, and W. Gao, *Carbon*, **118**, 443 (2017).
22. A. Moazami, M. Montazer, and M. K. Dolatabadi, *Fiber. Polym.*, **18**, 2287 (2017).
23. A. Moazami, M. Montazer, and M. K. Dolatabadi, *Fiber. Polym.*, **17**, 1359 (2016).
24. B. Ouadil, O. Cherkaoui, M. Safi, and M. Zahouily, *Appl. Surf. Sci.*, **414**, 292 (2017).
25. M. Mirjalili, *Fiber. Polym.*, **17**, 1579 (2016).
26. M. Ahmad, E. Ahmed, Z. L. Hong, J. F. Xu, N. R. Khalid, A. Elhissi, and W. Ahmed, *Appl. Surf. Sci.*, **274**, 273 (2013).
27. Y. Liu, Y. Hu, M. Zhou, H. Qian, and X. Hu, *Appl. Catal., B. Environ.*, **125**, 425 (2012).
28. J. Lin, M. Penchev, G. Wang, R. K. Paul, J. Zhong, X. Jing, M. Ozkan, and C. S. Ozkan, *Small*, **6**, 2448 (2010).
29. D. Fu, G. Han, F. Yang, T. Zhang, Y. Chang, and F. Liu, *Appl. Surf. Sci.*, **283**, 654 (2013).
30. S. S. Low, M. T. Tan, H. S. Loh, P. S. Khiew, and W. S. Chiu, *Anal. Chim. Acta*, **903**, 131 (2016).
31. B. Saravanakumar, R. Mohan, and S.-J. Kim, *Mater. Res. Bull.*, **48**, 878 (2013).
32. R. K. Upadhyay, N. Soin, and S. S. Roy, *RSC Adv.*, **4**, 3823 (2014).
33. A. A. Ashkarran and B. Mohammadi, *Appl. Surf. Sci.,* **342**, 112 (2015).
34. M. Shateri-Khalilabad and M. E. Yazdanshenas, *Cellulose*, **20**, 963 (2013).
35. Y. Feng, X. Zhang, Y. Shen, K. Yoshino, and W. Feng, *Carbohydr. Polym.*, **87**, 644 (2012).
36 F. Tavakoli, M. Salavati-Niasari, and F. Mohandes, *Mater. Res. Bull.*, **63**, 51 (2015).
37. H. Tapiero, K. D. Tew, G. N. Ba, and G. Mathe, *Biomed. Pharmacother.*, **56**, 200 (2002).
38. D. Klemm, B. Heublein, H. P. Fink, and A. Bohn, *Angew. Chem. Int. Ed.*, **44**, 3358 (2005).
39. C. B. Ong, L. Y. Ng, and A. W. Mohammad, *Renew. Sust. Energ. Rev.*, **81**, 536 (2018).
40. X. Liu, L. Pan, T. Lv, T. Lu, G. Zhu, Z. Sun, and C. Sun, *Catal. Sci. Technol.*, **1**, 1189 (2011).
41. V. R. Posa, V. Annavaram, J. R. Koduru, V. R. Ammireddy, and A. R. Somala, *Korean J. Chem. Eng.*, **33**, 456 (2016).
42. S. P. Lonkar, V. Pillai, and A. Abdala, *Appl. Surf. Sci.*, **465**, 1107 (2019).
43. X. Zou, L. Zhang, Z. Wang, and Y. Luo, *J. Am. Chem. Soc.*, **138**, 2064 (2016).
44. J. Li, G. Wang, H. Zhu, M. Zhang, X. Zheng, Z. Di, X. Liu, and X. Wang, *Sci. Rep.*, **4**, 4359 (2014).
45. F. Perreault, A. F. De Faria, S. Nejati, and M. Elimelech, *ACS Nano*, **9**, 7226 (2015).
46. T. Kavitha, A. I. Gopalan, K. P. Lee, and S. Y. Park, *Carbon*, **50**, 2994 (2012).
47. M. Shateri-Khalilabad and M. E. Yazdanshenas, *Carbohydr. Polym.*, **96**, 190 (2013).
48. B. Fugetsu, E. Sano, H. Yu, K. Mori, and T. Tanaka, *Carbon*, **48**, 3340 (2010).
49. K. M. McCreary, K. Pi, and R. K. Kawakami, *Appl. Phys. Lett.*, **98**, 192101 (2011).